



HAL
open science

ATP7B copper-regulated traffic and association with the tight junctions: copper excretion into the bile.

Sonia Hernandez, Yo Tsuchiya, Josefa P. García-Ruiz, Vassiliki Lalioti, Søren Nielsen, Doris Cassio, Ignacio V. Sandoval

► To cite this version:

Sonia Hernandez, Yo Tsuchiya, Josefa P. García-Ruiz, Vassiliki Lalioti, Søren Nielsen, et al.. ATP7B copper-regulated traffic and association with the tight junctions: copper excretion into the bile.: ATP7B and copper excretion by liver. *Gastroenterology*, 2008, 134 (4), pp.1215-23. 10.1053/j.gastro.2008.01.043 . inserm-00276812

HAL Id: inserm-00276812

<https://inserm.hal.science/inserm-00276812>

Submitted on 2 May 2008

HAL is a multi-disciplinary open access archive for the deposit and dissemination of scientific research documents, whether they are published or not. The documents may come from teaching and research institutions in France or abroad, or from public or private research centers.

L'archive ouverte pluridisciplinaire **HAL**, est destinée au dépôt et à la diffusion de documents scientifiques de niveau recherche, publiés ou non, émanant des établissements d'enseignement et de recherche français ou étrangers, des laboratoires publics ou privés.

Title. ATP7B copper-regulated traffic and association with the tight junctions: copper excretion into the bile

Short title. ATP7B and copper excretion by liver

Authors. Sonia Hernandez*[§], Yo Tsuchiya*[§], Josefa P.García-Ruiz*[§], Vassiliki Lalioti*, Søren Nielsen[&], Doris Cassio[¶] and Ignacio V. Sandoval*[&]

From the Centro de Biología Molecular Severo Ochoa. Consejo Superior de Investigaciones Científicas. Universidad Autónoma de Madrid. Cantoblanco 28049 Madrid. Spain*. Unité INSERM 442, Université Paris-Sud, Bâtiment 443, 91405 Orsay Cedex, France[¶]. The Water and Salt Research Center, University of Aarhus, Aarhus, Denmark[&].

[§]These authors contributed equally to this work

Grant support. This work was supported by grants of the Ministerio de Educacion y Ciencia from the Spanish Government (BFU-2005-07903; GEN2003-20662-C07-06) to I.V.S.

Abbreviations. Ab, antibody; Ap, apical plasma membrane; Bs, basolateral plasma membrane; TJ, tight junction; LIMP, lysosomal integral membrane protein; BCS, bathocuproine sulphate.

Correspondence to Ignacio V. Sandoval. Centro de Biología Molecular Severo Ochoa. Universidad Autónoma de Madrid. Cantoblanco Madrid 28049. Tel 914978455. FAX 914974799. e-mail: isandoval@cbm.uam.es

Financial Disclosures. None

Writing Assistance. San Francisco Edit

Abstract

The copper transporter ATP7B plays a central role in the elimination of excess copper by the liver into the bile, yet the site of its action remains controversial. Microscopy and cell fractionation studies of polarized CAN 10 cells forming long-branched bile canaliculi show that copper excess provokes a massive download of the ATP7B retained in the trans-Golgi network into the bile canalicular membrane. Furthermore, the bulk of ATP7B partitions with purified apical bile canalicular membrane. In addition, we localize a stable ATP7B pool to the tight junctions (TJs) that seal the bile canaliculi. The profile of Cu⁶⁴ excretion into the bile by isolated rat livers perfused under one-pass conditions provides evidence of copper excretion by two separate mechanisms, transcytosis across the hepatocyte and paracellular transport throughout the TJs. These results point that ATP7B functions in the bile canalicular membrane to excrete copper into the bile, provide evidence of the close association of an ATP7B pool with the TJs and indicate that copper is excreted into the bile by two separate pathways. The results are discussed in the frame of the normal and impeded excretion of copper into the bile.

Introduction

Bile constitutes the major route of copper excretion in vertebrates and represents the most important homeostatic mechanism determining the levels of the metal in the organism. Copper ions are exported from liver hepatocytes by a P-type copper ATP translocase, ATP7B (Cox, 1995). Under basal conditions (i.e. low copper levels) ATP7B is intracellularly sequestered in a compartment within the *trans*-Golgi (TGN) ^{1, 2}. ATP7B sequestration ends with the increase of cellular copper. However, the ultimate destination of released ATP7B is highly controversial. The early description of ATP7B translocation from the TGN to the bile canalicular membrane ³⁻⁵ has been challenged by a model that postulates the ATP7B target to late endosomes and the excretion of copper into the bile via the resulting ATP7B-free lysosomes ⁶⁻¹⁰ for a recent review see ¹⁰. The two models contemplate that under low copper levels the bulk of ATP7B is sequestered in the Golgi. Therefore an accurate description of the copper-regulated distribution of ATP7B in the hepatocyte is of great importance to understand how it responds to changes in copper levels and functions in the copper excretion through the bile.

Dysfunction of ATP7B disrupts copper homeostasis and is responsible for Wilson disease. Copper is poorly incorporated into ceruloplasmin at the Golgi when the translocase is defective ¹¹, excretion is diminished leading to the metal sequestration in lysosomes ¹², and typically a copper pan-toxicosis ensues severely damaging the liver and central nervous system. While the Wilson disease is Mendelian-linked to ATP7B, the ethiopathology of three hepatic copper toxicosis described in humans that are not Mendelian-linked to ATP7B remains unknown ¹³⁻¹⁵, pointing to our limited knowledge of the mechanisms that function in copper disposal in the liver.

We here describe that copper induces the massive translocation of intracellular ATP7B to the bile canalicular membrane in CAN 10 hepatoma cells. In addition, we localize a separate and stable pool of ATP7B at the hepatocyte TJs. Study of the rate of copper excretion by the bile in perfused rat livers provides evidence of the metal excretion by means of transcytosis through the hepatocyte and paracellular transport throughout the TJs.

Materials and Methods.

Cell lines. The CAN 10 a hepatoma cell line that upon polarization forms long tubular branched bile canaliculi and is competent for vectorial transport of organic anions and bile acids, was developed in the laboratory of Doris Cassio¹⁶. The cells were plated on plastic dishes or 10 mm coverglasses at a density of 3×10^4 cells/ml and cultured in F12 medium for 5-7 days.

Antibodies. ATP7B antibodies Ab1 and Ab2 were raised to the human N-cytoplasmic domain (aas 1-655) and to three synthetic peptides contained in the mouse ATP7B sequence (Q⁸³⁸-E⁸⁵², D¹²⁸⁹-S¹³¹³ and S¹³¹⁴-Q¹³⁴⁵), respectively (For more information on the development and specificity of the antibodies see Supporting Material Table I). Ab1 was raised in rabbit and mouse and Ab2 only in rabbit. The rabbit polyclonal anti-ATP7A antibody was developed against four synthetic peptides exclusively found in the human ATP7A sequence (p53-70, p139-163, p1411-1432, p1483-1500). The sequence homology between the N-domains (aas 38-655) of human ATP7B and ATP7A is shown in Suppl. Material. Mouse monoclonal antibodies to ZO-1 R26-4C¹⁷, HA4c19¹⁸ and MRP2[cMOAT]¹⁹ were used as markers of TJs and bile canalicular membrane, respectively. Mouse monoclonal antibody to Na⁺/K⁺ ATPase²⁰ was used as plasma membrane maker. Antibodies to lysosomal membrane proteins LIMPI and LIMPII²¹ trans-Golgi network GMP_{t-1}/TGN38^{22, 23}, syntaxin 6 (BD, Transduction laboratories), aquaporin 9 (AQ9A-1 Alpha Diagnostics) and GLUT4²⁴ were employed to study the cellular distribution of ATP7B under different conditions.

Chemicals. Bathocuproine sulphate (BCS) and CuCl₂ were from Sigma.

Preparation of cell, tissue lysates and fractions. Cell and tissue extracts were prepared in cold buffer A (20 mM Hepes pH 7.4, 0.25 M sucrose, 1 mM EDTA, 50 mM β-glycerophosphate, 50 mM NaF, 1 mM Na₃VO₄, 1 mM phenylmethylsulfonylfluoride, 5 μg/ml leupeptin, 5 μg/ml aprotinin and 1.5 μM pepstatin). Tissues were homogenized using a Potter Eveljhem. CAN 10 cells grown on p100 dishes were resuspended in 2 ml buffer A and passed twenty times through a cell cracker equipped with a 0.2500 in. diameter ball. Lysates were centrifuged for 5 min at 600 xg to remove nuclei and cell debris and whole membranes prepared by centrifugation for 90 min at 150.000xg. TGN and bile canaliculi rich fractions were prepared from CAN 10 cells as follows: Postnuclear supernatants were centrifuged at 20,000xg for 20 min using a TL100.3 rotor n a TL100 ultracentrifuge (Beckman) and the resulting pellet and supernatant used to purify bile canaliculi and LDM, respectively. To this end, the pellet was resuspended in 0.5 ml buffer A and laid over a 1 ml 35% sucrose cushion prepared in the same buffer and bile canaliculi collected by centrifugation for 1h at 108.000 xg using a swinging TLS 55 rotor. A fraction rich in TGN was separately collected by centrifugation of the 20,000xg supernatant for 90 min at 180,000xg. Apical (Ap) and basolateral (Bs) plasma membrane domains were subfractionated and purified from rat liver as described²⁵. By using this method we found that Ap membranes enriched in the HA4 marker floated on top of the 31% (w/w) sucrose cushion and the 31/34 % sucrose interphase and, as described, Bs membranes were recovered in the 34/38% sucrose interphase.

Immunofluorescence microscopy and Western analysis. All the experiments were performed using affinity purified ATP7B and ATP7A antibodies. Conventional and confocal immunofluorescence microscopy was performed as described before using an Axiovert 135M microscope (Zeiss) or a Bio-Rad Radiance 2000 microscope with the argon (488 nm) and helio/neon (543 nm) lasers set to 3 and

100, respectively, and with the iris aperture set to optimum. Typically, the cells were grown on 10 mm coverglasses for 48 h and fixed-permeabilized with cold (-20°C) methanol for 4 min. Alexa 488 and 647-conjugated goat anti-rabbit and anti-mouse IgGs (Invitrogen) were used as secondary antibodies. For Western analysis whole membranes were prepared by centrifugation of postnuclear supernatants at 150000xg for 90 min and the membrane proteins (100 µg), resolved by electrophoresis in 12 cm long SDS-10% or 8% polyacrylamide gels, were blotted into nitrocellulose and subjected to Western analysis using separately affinity-purified ATP7B and ATP7A antibodies diluted 1/500. Horseradish peroxidase (HRP) conjugated donkey anti-rabbit IgG was used as second antibody (GE Biomedicals).

Liver perfusion. 300 g male Wistar rats were anesthetised using 45 mg Ketolar, 0.5 mg valium and 0.1 mg atropine. Following bile duct cannulation, livers were isolated in situ and perfused at a constant flow rate of 15-17 ml/min with 150 ml of freshly prepared cell-free Krebs-Henseleit bicarbonate buffer, pH 7.4 (Krebs & Henseleit, 1932) containing 5 mM glucose, 2 mM glutamine, non essential aminoacids and 1% (w/v) bovine serum albumin (fraction V, Boehringer). The perfusion solution was recycled, gassed continuously with O₂/CO₂ (19: 1) and maintained at 37°C as described²⁶. 200 µCi Cu⁶⁴ (Nordion, Canada; specific activity 5 Ci/mg) or 50 µCi [³H] inulin (specific activity 0.5 mCi/mg) mixed with 4 mg HRP (Sigma type VI, prepared in solution the night before and kept at 4°C) were prepared in 0.3 ml perfusion medium and injected into the perfusion line just prior to the portal vein cannula. Immediately before the infusion, the perfusion circuit was opened, and the injection performed while collecting the medium surging from the liver (one-pass perfusion). Next, the organ was washed with 80 ml perfusion medium before closing the circuit and resuming the perfusion. Livers infused with Cu⁶⁴ were perfused with 1.1 mg CuCl₂/L. When required the livers were perfused for 90 min with 2 mM BCS and then, immediately before the Cu⁶⁴ infusion, were washed with 80 ml drug-free medium containing 1.1 mg/L CuCl₂ and the perfusion resumed with 2 mM BCS immediately after the Cu⁶⁴ infusion. The mean bile flow was 14 µl/min. Bile was collected every 2 min to measure the rates of Cu⁶⁴, [³H] inulin and HRP excretion. Cu⁶⁴ and [³H] inulin were measured using a LKB 1219 Rackbeta counter and the HRP activity colorimetrically as described²⁷.

Results.

Identification of ATP7B with specific antibodies. We developed two antibodies to ATP7B. Antibody-1 (Ab1), raised to the GST-N-ATP7B (aas 1-655) construct (for more details see Suppl. Material), reacted with ATP7B in liver and CAN 10 hepatoma cells, but also recognized the homologous and ubiquitous copper transporter ATP7A in tissues and cells of non-hepatocyte origin and as result recognized ATP7B and ATP7A in lysates of WIF B-9 cells, a hybrid of rat hepatoma-human fibroblasts, and in COS cells transfected with ATP7B (Figure 1). The reaction between Ab1 and ATP7B/ATP7A was abolished by preincubation of the antibody with GST-N-ATP7B. In contrast, antibody-2 (Ab2), which strongly recognized the extracellular loop linking the 5 and 6 transmembrane domains of ATP7B (see Suppl. Material), strictly reacted with ATP7B, the reaction being blocked by preincubation of the antibody with the peptides used for immunization (Fig 1).

ATP7B is massively translocated from the Golgi into the bile canalicular membrane in response to excess copper. To study the redistribution of ATP7B in response to an increase in copper levels we used CAN 10 cells, an hepatoma cell line that expressed only ATP7B and formed long-branched bile canaliculi upon polarization¹⁶. The cells were seeded at a density 3×10^4 cells/ml and cultured for 3 and 7 days, after which all were polarized but only the ones cultured for 7 days formed bile canaliculi. The copper response was studied by comparing the ATP7B distribution after cell treatment for 4h with 50- μ M BCS or 50 μ M CuCl_2 . Copper induced the vectorial translocation of ATP7B from the Golgi to the apical plasma membrane before (Fig 2, compare panels A, B) and after formation of bile canaliculi (Fig 2, compare panels C, D), the later an event that occurred by lateral displacement of their apical membrane domains¹⁶. Upon addition of 50 μ M CuCl_2 release of ATP7B from the Golgi was fast and within 2 min of the metal addition the transporter was partly relocated to punctuate structures, probably small vesicles, scattered throughout the cytoplasm (Suppl. Material Fig 1). Longer incubations with CuCl_2 resulted in substitution of the small vesicles by large ones preferentially localized at the edges of bile canaliculi (Suppl. Material Fig 1). Studies of vesicle biogenesis in non-polarized human hepatoma HepG2 cells, which characteristically retained all the transfected mouse ATP7B in vesicles, using Ab2 that exclusively recognized mouse ATP7B (see Suppl. Material text), showed that ATP7B-positive vesicles of medium and small size became in contact with each other to form larger vesicles (Suppl. Material Figure 2A1-3). This observation and the complete segregation of ATP7B and the lysosomal marker LIMPI in different vesicle populations (Suppl. Material Figure 2B) pointed that large ATP7B-loaded vesicles were mostly produced by homotypic fusion (see Discussion). Moreover, appearance of ATP7B in large vesicles and in the syntaxin/Rab11-positive subapical compartment (Suppl. Material Figure 1) preceded the massive download of ATP7B into the bile canalicular membrane, which flanked by the ZO-1 positive TJs was immunostained with antibodies against the apical membrane marker MRP2 (Figure 2D; Suppl. Material Figure 1E). The same result, massive translocation of ATP7B from the Golgi to the bile canalicular membranes, was observed when CAN 10 cells were first incubated for 2 h with 50 μ M BCS and after removal of the drug for 4h with 200 μ M CuCl_2 (not shown). Furthermore, in a reverse experiment, the wash out of copper and incubation with BCS dramatically reversed the

traffic direction and resulted in massive return and retention of ATP7B in the Golgi (Suppl. Material Figure 3). Altogether these results proved that excess copper induced the download of ATP7B into the bile canalicular membranes of fully polarized CAN 10 cells, and that upon decrease in copper levels the traffic direction was reversed and ATP7B returned from the bile canaliculi to the Golgi.

The sequestration of ATP7B in the Golgi of cells with low copper levels and the copper-induced download of ATP7B into the bile canaliculi was separately studied by cell fractionation experiments using CAN 10 cells incubated first for 4 h with 50 μ M BCS and then with 200 μ M CuCl_2 . The results showed that whereas the bulk of ATP7B was recovered with the TGN38-rich Golgi fraction of the cells treated with BCS, the addition of copper provoked the ATP7B translocation to the HA4-rich bile canalicular membrane fraction (Figure 3). Interestingly, we also observed in the same experiments that a significant amount of the t-SNARE involved in exocytosis syntaxin 6 was also translocated from the Golgi to the bile canalicular membrane enriched-fraction in response to increase in the copper levels (Figure 3). Therefore the microscopy and cell fractionation studies demonstrated that whereas ATP7B was sequestered in the Golgi of cells with low copper levels, excess copper provoked its massive download into the bile canalicular membrane.

ATP7B co-fractionates with hepatocyte apical plasma membrane. The translocation of ATP7B to the bile canalicular membrane of CAN 10 cells incubated with excess copper led us to compare the distribution of ATP7B between the apical (i. e. bile canalicular membrane) and basolateral domains of plasma membrane purified from rat liver. Western analysis showed that the bulk of the ATP7B associated with purified plasma membrane was recovered in the two HA4-rich apical membrane fractions separated from basolateral membrane and TGN elements by ultracentrifugation on a discontinuous sucrose gradient²⁵ (Figure 4). This result demonstrated the presence of ATP7B in the bile canalicular membrane of rat liver.

Localization of a stable ATP7B pool to the TJs of polarized CAN 10 cells and rat liver. Current models of ATP7B distribution and trafficking in hepatocytes describe a homogeneous pool of ATP7B molecules that responds uniformly to changes in copper levels. Yet, we observed in CAN 10 cells treated for 4h with 50 μ M BCS and stained with Ab2 that in addition to the expected retention of ATP7B in the Golgi, the antibody also reacted strongly with the TJs flanking the bile canalicular membranes (Figure 5A, 5B). Furthermore, the staining of the TJs by Ab2 was comparable after treatment of the cells for 4h with 50 μ M CuCl_2 (Figure 5C, 5D). These observations and the specific reaction of Ab2 with ATP7B (Figure 1)emonstated the association of a population of ATP7B molecules with the TJs. Interestingly, in striking contrast with Ab1, Ab2 did not react with the ATP7B translocated to the bile canalicular membrane (Figure 5C, 5D) and as result double-staining of bile canaliculi by Ab1 and Ab2 was complementary in cells treated with excess CuCl_2 (Figure 5M-P). Next, we studied the distribution of ATP7B in rat liver slices stained with Ab2. In agreement with the results of the CAN 10 studies, Ab2 specifically stained the hepatocytes TJs as showed the examination of en-face and cross-sections of bile canaliculi, thus confirming the association of ATP7B with the TJs observed in the CAN 10 cell studies (Figure 6).

Copper is excreted into the bile by separate paracellular and transcellular mechanisms. Since ions are transported from blood into the bile by transcytosis and paracellular transport through the TJs, next we studied the mechanisms of copper excretion into the bile by monitoring its appearance in the bile after infusion of Cu^{64} into the portal vein of perfused liver. The study was performed operating under one-pass conditions. We found that the excretion time of a substantial amount of Cu^{64} coincided with the first wave of HRP and slightly preceded the elimination of inulin, two markers of the paracellular transport across the TJs²⁸ (compare Figures 7A and B). In three separate experiments the early wave of Cu^{64} in the bile was detected 9 min after its infusion and peaked 9 min later. This first wave clearly preceded a second one that lasted longer and partly overlapped with the wave of HRP excreted after transcytosis through the hepatocyte²⁸ (compare Figures 7B and A). Furthermore, whereas the first wave of excreted Cu^{64} was unaffected by a 90 min liver perfusion with 2 mM BCS (treatment aimed to remove ATP7B from the bile canalicular membrane and induced its sequestration in the Golgi), the copper-chelator treatment dramatically decreased the amplitude of the second wave (Figure 7B). This result and the sequestration of ATP7B in the Golgi of the cells treated with BCS (Figures 2 and 5) pointed that the second wave was made up by the copper excreted by transcytosis through the bile canalicular membrane. Altogether these observations strongly indicated that copper was excreted into the bile by separate paracellular and transcellular mechanisms.

Discussion.

Our studies provide evidence for the existence of two separate pools of ATP7B in the membranes of bile caniculi and hepatocyte TJs and show that excretion of copper by the liver into the bile occurs by separate paracellular and transcellular mechanisms.

The initial description in HepG2 cells incubated with copper of the downregulation of ATP7B into the bile canaliculi³ has been followed by results that put forwards a model that excludes ATP7B from the bile canaliculi and describes biliary copper excretion as result of the ATP7B-mediated pumping of copper into endosomes and the subsequent fusion of copper-loaded lysosomes with the canalicular membrane^{8, 9, 29, 30}. Furthermore, reports that ATP7B does not traffic to the plasma membrane of fibroblasts treated with copper appear to fit with the observations made in hepatoma cells⁹. However, partial localization of ATP7B at the apical membrane of WIF-B9 cells after treatment with copper has been also reported³¹ and more recently the lining of bile canaliculi with ATP7B-positive vesicles in HepG2 cells has been discussed as proof of the transient presence of small amounts of ATP7B in the bile canalicular membrane³². Our studies of CAN 10 cells show that ATP7B is massively translocated from the Golgi to the bile canaliculi upon increase in copper levels, thus confirming the results from the Vonk's laboratory. The massive presence of ATP7B in the bile canalicular membrane of cells incubated with excess copper strongly suggests that ATP7B functions in the canalicular membrane to pump out copper into the bile. Moreover, contrary to the results of previous studies of hepatoma cells incubated with copper the amount of ATP7B retained in the Golgi was minimal. Pouring of ATP7B into the bile canalicular membrane of CAN 10 cells treated with copper has been assessed by demonstration of its codistribution with the bile canalicular membrane markers MRP2 and HA4 as well as by the flanking of the ATP7B-positive membranes by the TJs marker ZO-1.

Is striking the contrast between the ability of Ab1 to recognize both the ATP7B molecules retained in the Golgi and translocated to the bile canalicular membrane, and the restricted reaction of Ab2 with those retained in Golgi and TJs. The indistinguishable reaction of Ab1 and Ab2 with blotted ATP7B protein and their different reactivity with the protein in situ point to an existing correlation between reactivity and location that may result from epitope masking, probably due to ATP7B modifications or its interaction with other proteins at specific locations.

The existence of two separate pools of ATP7B, one trafficking in a copper regulated manner between the Golgi and bile canaliculi and a second that appears more stable in the TJs, raises the question of the relationship between ATP7B location and function. Whether the ATP7B retained in the TJs is involved in paracellular transport of copper into the bile is nevertheless uncertain. The question is however pertinent since the time coincidence between the paracellular excretion of HRP and inulin and the appearance of the first wave of infused Cu⁶⁴ in the bile points that a significant amount of copper is paracellularly transported into the bile. Furthermore, this conclusion is strongly supported by the insensitivity of the copper co-excreted with inulin to pretreatment of the liver with BCS, treatment that strongly inhibits the second wave of excreted copper transported through the hepatocyte. Whereas active transporters and pumps function in the transcellular transport of organic compounds and ions into the bile, paracellular transport through TJs has been firmly demonstrated to result from passive movement of solutes and water down electrochemical gradients through claudin-based barriers³³. Transport of ions

both by paracellular and transcellular mechanisms is not an uncommon phenomenon and has been explained by the saturation of cellular transporters and the lack of saturation of the paracellular pathway over a large concentration range. Involvement of ATP7B in the paracellular transport of copper would require its reorientation in a position perpendicular to that of the molecules retained in the plasma membrane with the copper binding sites exposed on the lumen of the blood sinusoids. Furthermore, the ubiquitiveness of the claudin barriers would require insertion of ATP7B within the structural framework made of the claudins pores. Alternatively, the ATP7B pump lodged in the claudin barriers at the TJs might function either as a safe-valve to maintain intracellular copper below toxic levels under basal conditions or as part of a copper-based mechanism that regulates the functioning of TJs. With regard to this, is interesting the regulation of paracellular permeability by the unconventional complex Kir6.1-SUR2A, two members of the inwardly rectifying K⁺ channels³⁴. As the K⁺ channels in the cerebellar pinceaux³⁵ ATP7B channels in the apical side of the TJs appear to attribute a positive charge to the inner claudins and as result decrease the influx of cations and increase the efflux of anions through the claudin pores. Although lack of claudin-1 expression in cholangiocytes is known to result in bile duct injury³⁶, whether the lack of the claudins that flank the bile canaliculi have a similar effect is unknown. Since the mixing ratios of claudins in a given type of cell appear to determine barrier property in terms of charge selectivity, new information could be critical to understand how ATP7B channels may function to regulate paracellular transport in liver. Furthermore, and not mutually exclusive, being the backbone of TJs made by claudins connected to scaffolds that transmit regulatory signals and fasten the claudins to the cytoskeleton³⁷, the interaction of ATP7B with the ZO-1 scaffold (our unpublished results) raises the possibility that it may act as a transducer that couples changes in copper levels to structural and functional changes in the TJs. Also not known is if the copper excreted through the paracellular pathway is or not bound to albumin or histidine, carriers that due to the running of the portal vein from the intestine to the liver may have not time to react efficiently with all the copper absorbed from the diet.

The functioning of ATP7B in the TJs and the ability of the MURR1 protein to inhibit NF-κB and as result stimulate the synthesis of claudin 2, occludins and the TJs stabilizer connexin 32^{38, 39} may explain the copper toxicosis linked to COMMD1/Murr1 gene in Bedlington foxterriers^{40, 41}. With regard to ATP7B dysfunction and disease it would be interesting to know if TJ dysfunction is implicated in some of the three non-Wilsonian copper toxicosis described in humans¹³⁻¹⁵.

Figure legends.

Figure 1. Antibodies Ab1 and Ab2 reaction with ATP7B. (A) Reactivity of Ab1 and Ab2 with the corresponding immunogens GST-human N-ATP7B (M¹-L⁶⁵⁵) and mouse ATP7B (Q⁸³⁸-E⁸⁵²; D¹²⁸⁹-S¹³¹³, S¹³¹⁴-Q¹³⁴⁵), respectively; antibody reactivity was measured by ELISA. (For more details see Suppl. Material). (B) Reaction specificity of Ab1 and Ab2. Whole postnuclear membranes (100 µg) from tissues and cells were subjected to Western analysis using affinity-purified Ab1 and Ab2. When indicated Ab1 was preincubated overnight at 4°C with 20 µg of the corresponding immunogens (+ N-ATP7B, + ATP7B pept.). Note the reaction of Ab1 with ATP7B (▷) and ATP7A (▶) and, in contrast, the exclusive reaction of Ab2 with ATP7B. The * marked protein was an ATP7B proteolytic product that increased with sample manipulation and storage.

Figure 2. Copper induced translocation of ATP7B from the Golgi to the bile canalicular membrane. Polarized CAN 10 cells grown in differentiation medium for 3 and 7 days and without (A, B) and with bile canaliculi (C, D) were incubated for 4 h with either 50 µM BCS (A, C) or 50 µM CuCl₂ (B, D). After fixation-permeabilization the cells were double-immunostained for ATP7B with Ab1 (FITC) and for the TJ protein ZO-1 with antibody R26-4C (Texas red). Note in cells treated with BCS that the bulk of ATP7B was retained in the Golgi (panel A1, A2, arrowheads; A3 orthogonal viewing of z-series stacks, arrowhead; panel C1, C2 arrowheads) as well as the exclusion of ATP7B from long (C1 double-arrowhead, C3; orthogonal viewing of z-series stacks) and short bile canaliculi with the typical lariat morphology (C1, C4 arrows). Observe that after treatment with CuCl₂ the bulk of ATP7B was released from the Golgi and found in vesicles (B4, D2, arrowheads) and in the apical plasma membrane (compare A3 and B3, C3 and D3; orthogonal viewing of z-series stacks): note the codistribution of ATP7B and ZO-1 in the plasma membrane of cells without bile canaliculi (compare A1, A3 and B1, B3) and how ATP7B was translocated to the membrane of large (compare C1, D1, double arrowheads; C3 and D3 orthogonal viewing of z-series stacks) and small bile canaliculi (compare C1, D1; C4, D4, arrows) flanked by ZO-1. Bars 15 µm, except in panels C3 and D3 that were 75 µm.

Figure 3. ATP7B partitioning between TGN and bile canaliculi-enriched fractions from CAN 10 cells is copper-dependent. Polarized CAN 10 cells incubated for 4h with 50 µM bathocuproine (BCS) and after washing out the drug treated with 200 µM CuCl₂ were fractionated to separate the TGN sequestration compartment and the bile canaliculi (BC) (see Materials and Methods). TGN38 and HA4 were used as markers of TGN and bile canalicular membranes, respectively. Syntaxin 6, a t-SNARE that is released together with ATP7B from the TGN in response to increased copper levels, was used to double-check the copper response. Observe that the bulk of ATP7B was recovered in the TGN38/syntaxin 6-rich TGN fraction of cells treated with BCS and that a small but significant amount was recovered in the HA4-positive bile canalicular fraction. Confirming the results of microscopy studies (Figure 2) excess copper decreased the levels of ATP7B and syntaxin 6 in the TGN fraction and increased their levels in the bile canaliculi-rich fraction. Preincubation of Ab1 with the N-ATP7B immunogen inhibited the Ab1 reaction with ATP7B.

Figure 4. ATP7B is recovered with apical plasma membrane purified from rat liver. The distribution of ATP7B and the markers of bile canaliculi HA4, plasma membrane Na⁺/K⁺ ATPase and *trans*-Golgi TGN38 were scrutinized in apical (Ap1 and Ap2) and basolateral (Bs) plasma membrane-enriched fractions purified from normal rat liver. TGN38 was also studied in whole membranes (WM). 10 μg (3 first lanes) and 20 μg of membrane protein (3 last lanes) were resolved by electrophoresis in SDS-PAGE using 8% polyacrylamide and after their blotting onto nitrocellulose subjected to Western analysis using specific antibodies. Note the accumulation of ATP7B in the HA4-enriched/TGN38 poor Ap1 and Ap2 fractions and its exclusion from the Bs fraction. Whole purified plasma membrane and apical and basolateral plasma membrane fractions were lysosomes-free as shown by the lack of the lysosomal marker LIMP2²¹ in the three plasma membrane fractions (not shown).

Figure 5. Localization of ATP7B to ZO-1 positive TJs. CAN 10 cells grown for 7 days in differentiation medium were incubated for 4 h with either 200 μM BCS (A, B) or 200 μM CuCl₂ (C, D). The fixed-permeabilized cells were double-immunostained with rabbit polyclonal Ab2 (FITC) and either the mouse monoclonal to ZO-1 or the mouse polyclonal Ab1 (Texas red) as indicated in the panels. The images shown in panels 2-4 are magnifications of areas containing the Golgi or bile canaliculi. Panels 3 show orthogonal views of z-series stacks taken at the sites marked with white bars. Note the retention of ATP7B in the perinuclear area (i.e. Golgi) of cells treated with BCS (A1, A2, B1, B2, arrowheads). Observe the staining of the ZO-1-positive TJs flanking long and short bile canaliculi with Ab2 and how the staining was unaffected by the changes in the levels of copper (Compare A, N and C, D). Note the staining of the Golgi by Ab1 and Ab2 in cells treated with BCS (A, B) and the negligible reaction of Ab2 with the bile canalicular membrane in cells treated with copper (C, D). Bars: A11 bars 15 μm, except C3, 51 μm; B2, D4, 7.5 μm; B3, 38 μm; D3, 60 μm.

Figure 6. ATP7B is found in the TJs of rat liver. Sections from normal rat liver were immunostained for ATP7B, TGN and basolateral aquaporine 9 as indicated in the panels using as second antibodies FITC, Texas red and HRP-conjugated rabbit and mouse IgGs. Note the strong staining of the bile canaliculi walls in both en face and cross section views (A, magnified in B; C). Observe the distribution of TGN dictyosomes along the bile canaliculi (A, B) and the failure of Ab2 to stain the ATP7B associated with the bile canalicular membrane (A, B, C). Note that surface staining of hepatocytes by Ab2 and the antibody to aquaporine 9 were complementary (C, D). Preincubation of Ab2 with the 3 peptides used as immunogens (2 μg/ μl) inhibited the bile canaliculi staining (i.e. TJ) (panel E). Bars 15 μm.

Figure 7. Copper is excreted by liver into the bile through separate paracellular and transcellular mechanisms Isolated perfused rat livers were infused with [³H]Inulin (100 μCi, specific activity 0.5 mCi/mg ■), HRP (4.5 mg ◆) or ⁶⁴Cu (0.25 mCi, specific activity 5 Ci/mg ◆ ■) at time zero (infusion time 15 sec; volume infused 0.3 ml) under one-pass conditions. When required the livers were perfused with 2 mM BCS before (90 min) and after the ⁶⁴Cu infusion (for details see Materials and Methods).

Bile samples were collected from the bile duct every 2 min after the infusions. Taking into account the volume of the bile duct cannula (123 μ l), the mean bile flow of 14 μ l /min, and the 35 μ l volume of the biliary tree ⁴² there was a delay in these experiments of about 6-7 min between the entrance of ⁶⁴Cu, inulin and HRP in the bile canaliculi and their appearance in the bile samples. The experiments shown are representative of three separate experiments.

Acknowledgments: We are very grateful to Dr. Luis Alvarez (Molecular Biology Division, Hospital Universitario La Paz, Madrid) for providing the facilities for liver perfusion experiments and to Dr. S. Lutsenko for lending us an antibody to ATP7B that helped us to double-check the results obtained with our Ab1 antibody .

References

1. Bingham MJ, Ong TJ, Ingledew WJ, McArdle HJ. ATP-dependent copper transporter, in the Golgi apparatus of rat hepatocytes, transports Cu(II) not Cu(I). *Am J Physiol* 1996;271:G741-6.
2. Yang XL, Miura N, Kawarada Y, Terada K, Petrukhin K, Gilliam T, Sugiyama T. Two forms of Wilson disease protein produced by alternative splicing are localized in distinct cellular compartments. *Biochem J* 1997;326 (Pt 3):897-902.
3. Roelofsen H, Wolters H, Van Luyn MJ, Miura N, Kuipers F, Vonk RJ. Copper-induced apical trafficking of ATP7B in polarized hepatoma cells provides a mechanism for biliary copper excretion. *Gastroenterology* 2000;119:782-93.
4. Ihrke G, Neufeld EB, Meads T, Shanks MR, Cassio D, Laurent M, Schroer TA, Pagano RE, Hubbard AL. WIF-B cells: an in vitro model for studies of hepatocyte polarity. *J Cell Biol* 1993;123:1761-75.
5. Fanni D, Pilloni L, Orru S, Coni P, Liguori C, Serra S, Lai ML, Uccheddu A, Contu L, Van Eyken P, Faa G. Expression of ATP7B in normal human liver. *Eur J Histochem* 2005;49:371-8.
6. Harada M, Sakisaka S, Terada K, Kimura R, Kawaguchi T, Koga H, Taniguchi E, Sasatomi K, Miura N, Sukanuma T, Fujita H, Furuta K, Tanikawa K, Sugiyama T, Sata M. Role of ATP7B in biliary copper excretion in a human hepatoma cell line and normal rat hepatocytes. *Gastroenterology* 2000;118:921-8.
7. La Fontaine S, Theophilos MB, Firth SD, Gould R, Parton RG, Mercer JF. Effect of the toxic milk mutation (tx) on the function and intracellular localization of Wnd, the murine homologue of the Wilson copper ATPase. *Hum Mol Genet* 2001;10:361-70.
8. Schaefer M, Hopkins RG, Failla ML, Gitlin JD. Hepatocyte-specific localization and copper-dependent trafficking of the Wilson's disease protein in the liver. *Am J Physiol* 1999;276:G639-46.
9. Cater MA, La Fontaine S, Shield K, Deal Y, Mercer JF. ATP7B mediates vesicular sequestration of copper: insight into biliary copper excretion. *Gastroenterology* 2006;130:493-506.
10. Lutsenko S, Barnes NL, Bartee MY, Dmitriev OY. Function and regulation of human copper-transporting ATPases. *Physiol Rev* 2007;87:1011-46.
11. Cox DW. Genes of the copper pathway. *Am J Hum Genet* 1995;56:828-34.
12. Mohan P, Failla M, Bremner I, Arthur-Smith A, Kerzner B. Biliary copper excretion in the neonatal rat: role of glutathione and metallothionein. *Hepatology* 1995;21:1051-7.
13. Wijmenga C, Muller T, Murli IS, Brunt T, Feichtinger H, Schonitzer D, Houwen RH, Muller W, Sandkuijl LA, Pearson PL. Endemic Tyrolean infantile cirrhosis is not an allelic variant of Wilson's disease. *Eur J Hum Genet* 1998;6:624-8.
14. Muller T, van de Sluis B, Muller W, Pearson P, Wijmenga C. Non-Indian childhood cirrhosis. *Eur J Med Res* 1999;4:293-7.
15. Maggiore G, De Giacomo C, Sessa F, Burgio GR. Idiopathic hepatic copper toxicosis in a child. *J Pediatr Gastroenterol Nutr* 1987;6:980-3.
16. Peng X, Grosse B, Le Tiec B, Nicolas V, Delagebeaudeuf C, Bedda T, Decaens C, Cassio D. How to induce non-polarized cells of hepatic origin to express typical hepatocyte polarity: generation of new highly polarized cell models

- with developed and functional bile canaliculi. *Cell Tissue Res* 2006;323:233-43.
17. Stevenson BR, Siliciano JD, Mooseker MS, Goodenough DA. Identification of ZO-1: a high molecular weight polypeptide associated with the tight junction (zonula occludens) in a variety of epithelia. *J Cell Biol* 1986;103:755-66.
 18. Bartles JR, Braiterman LT, Hubbard AL. Endogenous and exogenous domain markers of the rat hepatocyte plasma membrane. *J Cell Biol* 1985;100:1126-38.
 19. Paulusma CC, Kothe MJ, Bakker CT, Bosma PJ, van Bokhoven I, van Marle J, Bolder U, Tytgat GN, Oude Elferink RP. Zonal down-regulation and redistribution of the multidrug resistance protein 2 during bile duct ligation in rat liver. *Hepatology* 2000;31:684-93.
 20. Lebovitz RM, Takeyasu K, Fambrough DM. Molecular characterization and expression of the (Na⁺ + K⁺)-ATPase alpha-subunit in *Drosophila melanogaster*. *Embo J* 1989;8:193-202.
 21. Barriocanal JG, Bonifacino JS, Yuan L, Sandoval IV. Biosynthesis, glycosylation, movement through the Golgi system, and transport to lysosomes by an N-linked carbohydrate-independent mechanism of three lysosomal integral membrane proteins. *J Biol Chem* 1986;261:16755-63.
 22. Yuan L, Barriocanal JG, Bonifacino JS, Sandoval IV. Two integral membrane proteins located in the cis-middle and trans-part of the Golgi system acquire sialylated N-linked carbohydrates and display different turnovers and sensitivity to cAMP-dependent phosphorylation. *J Cell Biol* 1987;105:215-27.
 23. Alcalde J, Egea G, Sandoval IV. gp74 a membrane glycoprotein of the cis-Golgi network that cycles through the endoplasmic reticulum and intermediate compartment. *J Cell Biol* 1994;124:649-65.
 24. Martinez-Arca S, Lalioti VS, Sandoval IV. Intracellular targeting and retention of the glucose transporter GLUT4 by the perinuclear storage compartment involves distinct carboxyl-tail motifs. *J Cell Sci* 2000;113 (Pt 10):1705-15.
 25. Meier PJ, Sztul ES, Reuben A, Boyer JL. Structural and functional polarity of canalicular and basolateral plasma membrane vesicles isolated in high yield from rat liver. *J Cell Biol* 1984;98:991-1000.
 26. Hems R, Ross BD, Berry MN, Krebs HA. Gluconeogenesis in the perfused rat liver. *Biochem J* 1966;101:284-92.
 27. Pinna MC, Bauduin P, Touraud D, Monduzzi M, Ninham BW, Kunz W. Hofmeister effects in biology: effect of choline addition on the salt-induced super activity of horseradish peroxidase and its implication for salt resistance of plants. *J Phys Chem B Condens Matter Mater Surf Interfaces Biophys* 2005;109:16511-4.
 28. Lowe PJ, Kan KS, Barnwell SG, Sharma RK, Coleman R. Transcytosis and paracellular movements of horseradish peroxidase across liver parenchymal tissue from blood to bile. Effects of alpha-naphthylisothiocyanate and colchicine. *Biochem J* 1985;229:529-37.
 29. Harada M, Kawaguchi T, Kumemura H, Terada K, Ninomiya H, Taniguchi E, Hanada S, Baba S, Maeyama M, Koga H, Ueno T, Furuta K, Suganuma T, Sugiyama T, Sata M. The Wilson disease protein ATP7B resides in the late endosomes with Rab7 and the Niemann-Pick C1 protein. *Am J Pathol* 2005;166:499-510.
 30. Harada M, Kumemura H, Sakisaka S, Shishido S, Taniguchi E, Kawaguchi T, Hanada S, Koga H, Kumashiro R, Ueno T, Suganuma T, Furuta K, Namba M, Sugiyama T, Sata M. Wilson disease protein ATP7B is localized in the late

- endosomes in a polarized human hepatocyte cell line. *Int J Mol Med* 2003;11:293-8.
31. Guo Y, Nyasae L, Braiterman LT, Hubbard AL. NH₂-terminal signals in ATP7B Cu-ATPase mediate its Cu-dependent anterograde traffic in polarized hepatic cells. *Am J Physiol Gastrointest Liver Physiol* 2005;289:G904-16.
 32. Barte MY, Lutsenko S. Hepatic copper-transporting ATPase ATP7B: function and inactivation at the molecular and cellular level. *Biometals* 2007;20:627-37.
 33. Van Itallie CM, Anderson JM. Claudins and epithelial paracellular transport. *Annu Rev Physiol* 2006;68:403-29.
 34. Jons T, Wittschieber D, Beyer A, Meier C, Brune A, Thomzig A, Ahnert-Hilger G, Veh RW. K⁺-ATP-channel-related protein complexes: potential transducers in the regulation of epithelial tight junction permeability. *J Cell Sci* 2006;119:3087-97.
 35. Laube G, Roper J, Pitt JC, Sewing S, Kistner U, Garner CC, Pongs O, Veh RW. Ultrastructural localization of Shaker-related potassium channel subunits and synapse-associated protein 90 to septate-like junctions in rat cerebellar Pinceaux. *Brain Res Mol Brain Res* 1996;42:51-61.
 36. Hadj-Rabia S, Baala L, Vabres P, Hamel-Teillac D, Jacquemin E, Fabre M, Lyonnet S, De Prost Y, Munnich A, Hadchouel M, Smahi A. Claudin-1 gene mutations in neonatal sclerosing cholangitis associated with ichthyosis: a tight junction disease. *Gastroenterology* 2004;127:1386-90.
 37. Shin K, Fogg VC, Margolis B. Tight junctions and cell polarity. *Annu Rev Cell Dev Biol* 2006;22:207-35.
 38. Soler AP, Marano CW, Bryans M, Miller RD, Garulacan LA, Mauldin SK, Stamato TD, Mullin JM. Activation of NF-kappaB is necessary for the restoration of the barrier function of an epithelium undergoing TNF-alpha-induced apoptosis. *Eur J Cell Biol* 1999;78:56-66.
 39. Yamamoto T, Kojima T, Murata M, Takano K, Go M, Chiba H, Sawada N. IL-1beta regulates expression of Cx32, occludin, and claudin-2 of rat hepatocytes via distinct signal transduction pathways. *Exp Cell Res* 2004;299:427-41.
 40. Klomp AE, van de Sluis B, Klomp LW, Wijmenga C. The ubiquitously expressed MURR1 protein is absent in canine copper toxicosis. *J Hepatol* 2003;39:703-9.
 41. van de Sluis BJ, Breen M, Nanji M, van Wolferen M, de Jong P, Binns MM, Pearson PL, Kuipers J, Rothuizen J, Cox DW, Wijmenga C, van Oost BA. Genetic mapping of the copper toxicosis locus in Bedlington terriers to dog chromosome 10, in a region syntenic to human chromosome region 2p13-p16. *Hum Mol Genet* 1999;8:501-7.
 42. Olson JR, Fujimoto JM, Peterson RE. Three methods for measuring the increase in the capacity of the distended biliary tree in the rat produced by alpha-naphthylisothiocyanate treatment. *Toxicol Appl Pharmacol* 1977;42:33-43.

Figure 1

A

	ELISA reactivity			
	GST-M ¹ -L ⁶⁵⁵	Q ⁸³⁸ -E ⁸⁵²	D ¹²⁸⁹ -S ¹³¹³	S ¹³¹⁴ -Q ¹³⁴⁵
ATP7B Ab1	+++++	-	-	-
ATP7b Ab2	-	+++++	+	++

B

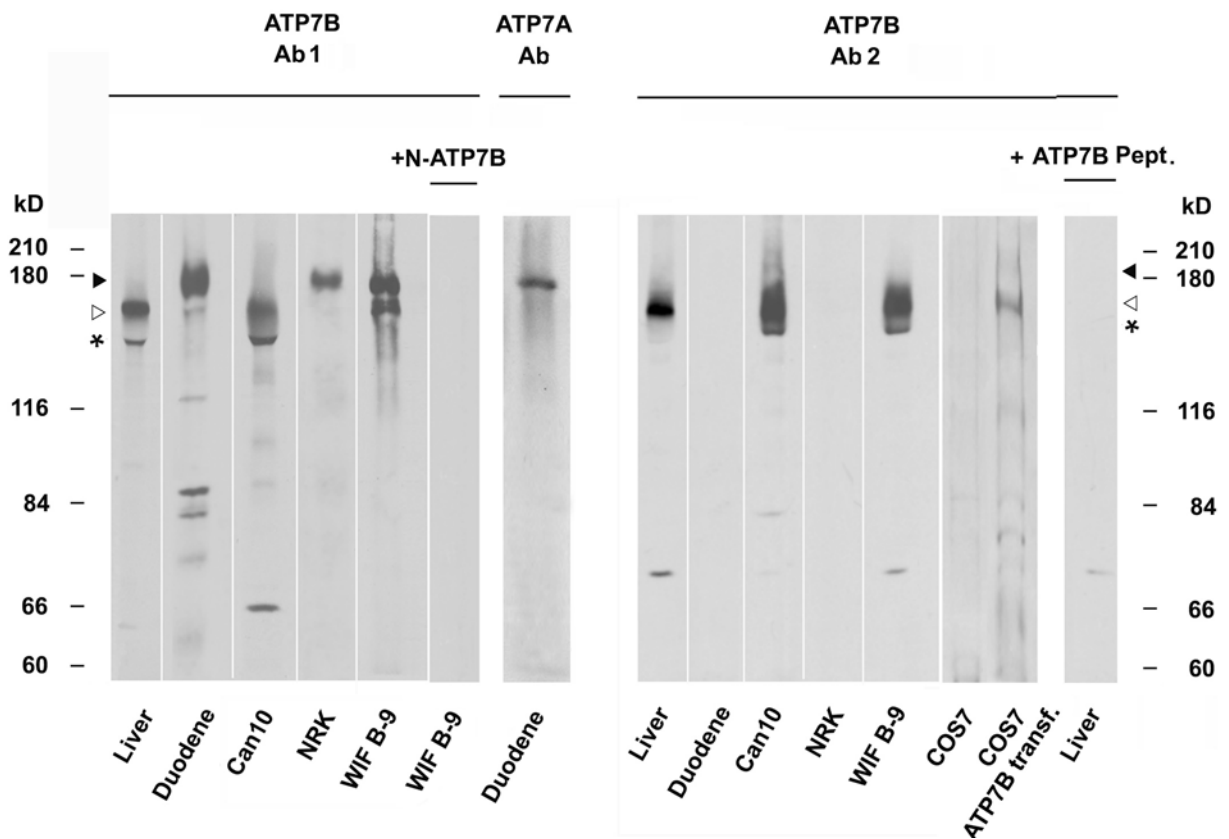


Figure 2

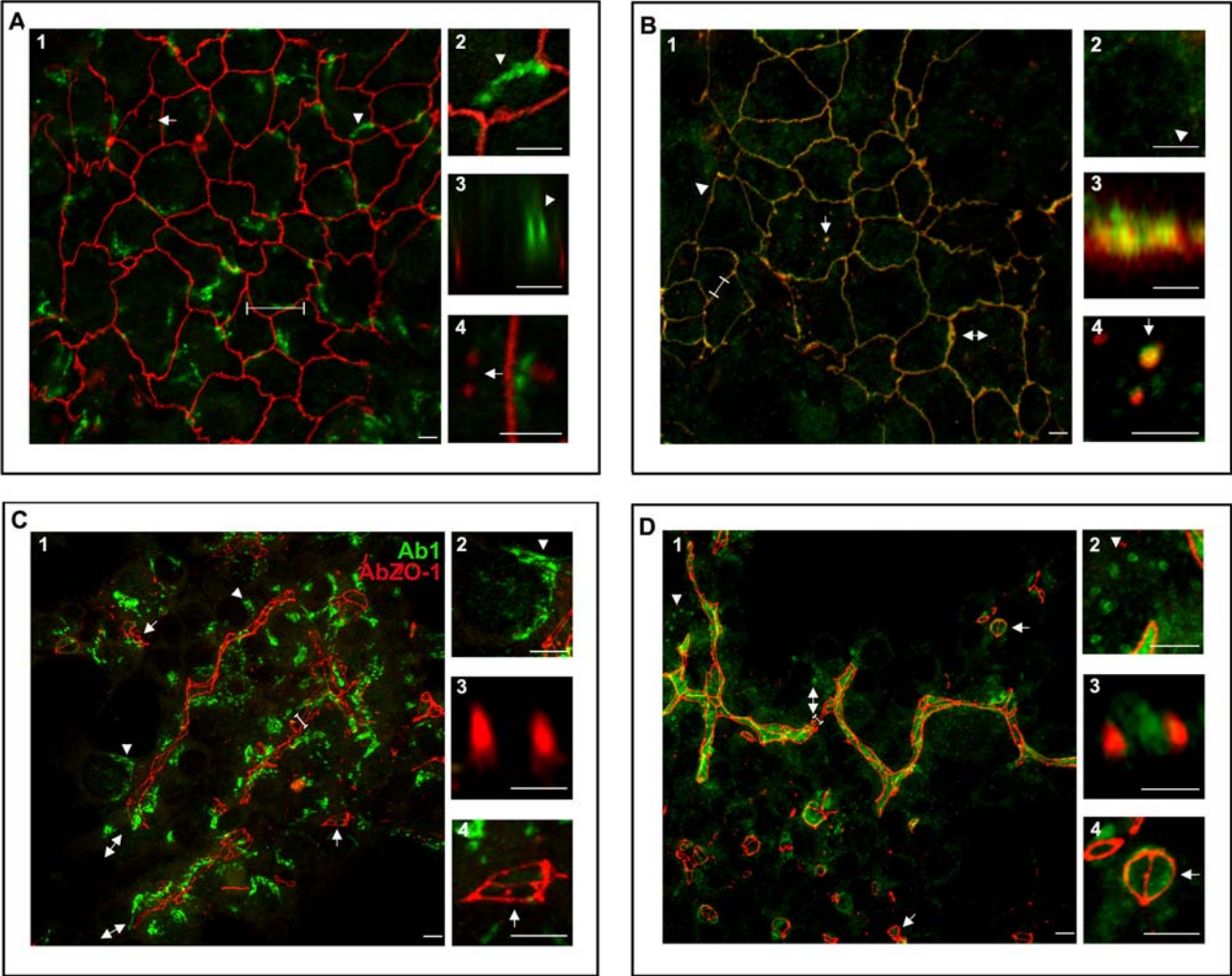


Figure 3

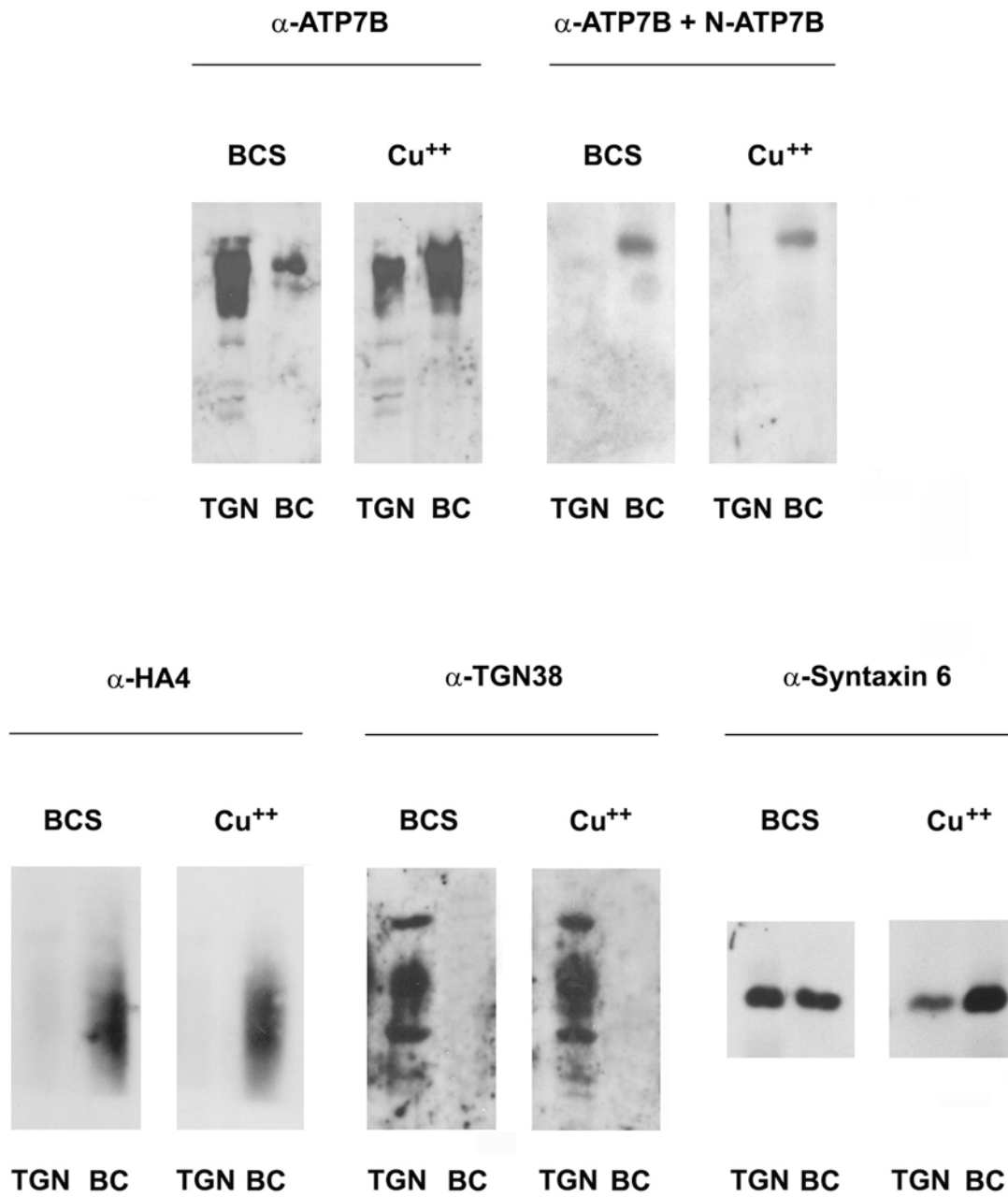


Figure 5

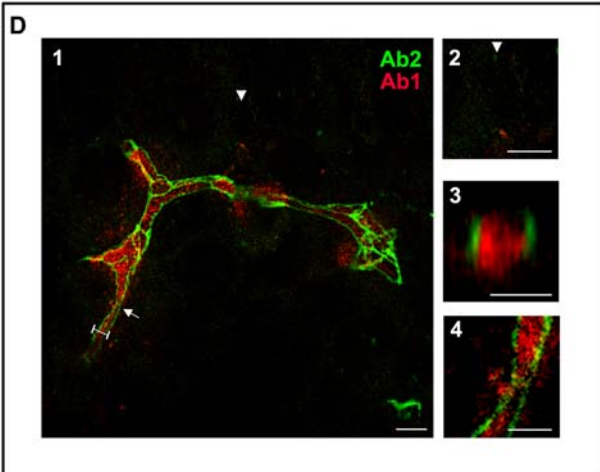
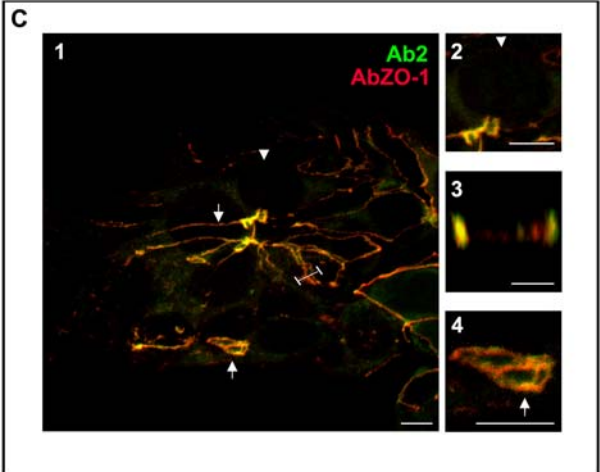
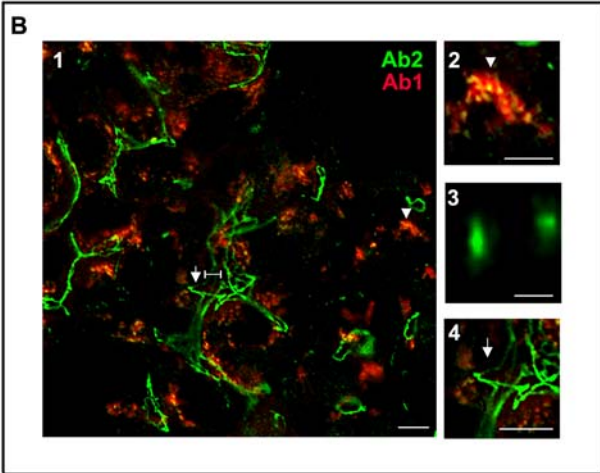
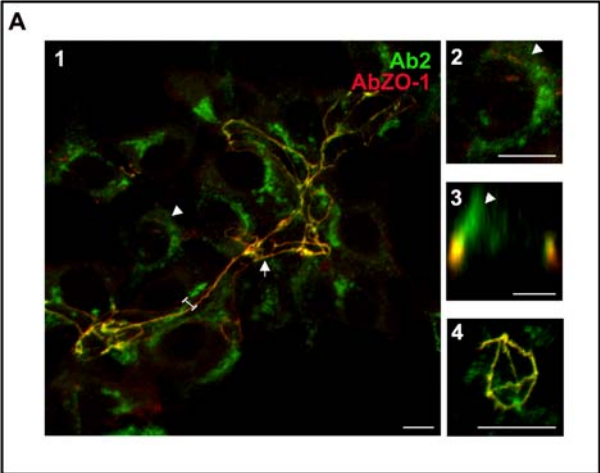


Figure 6

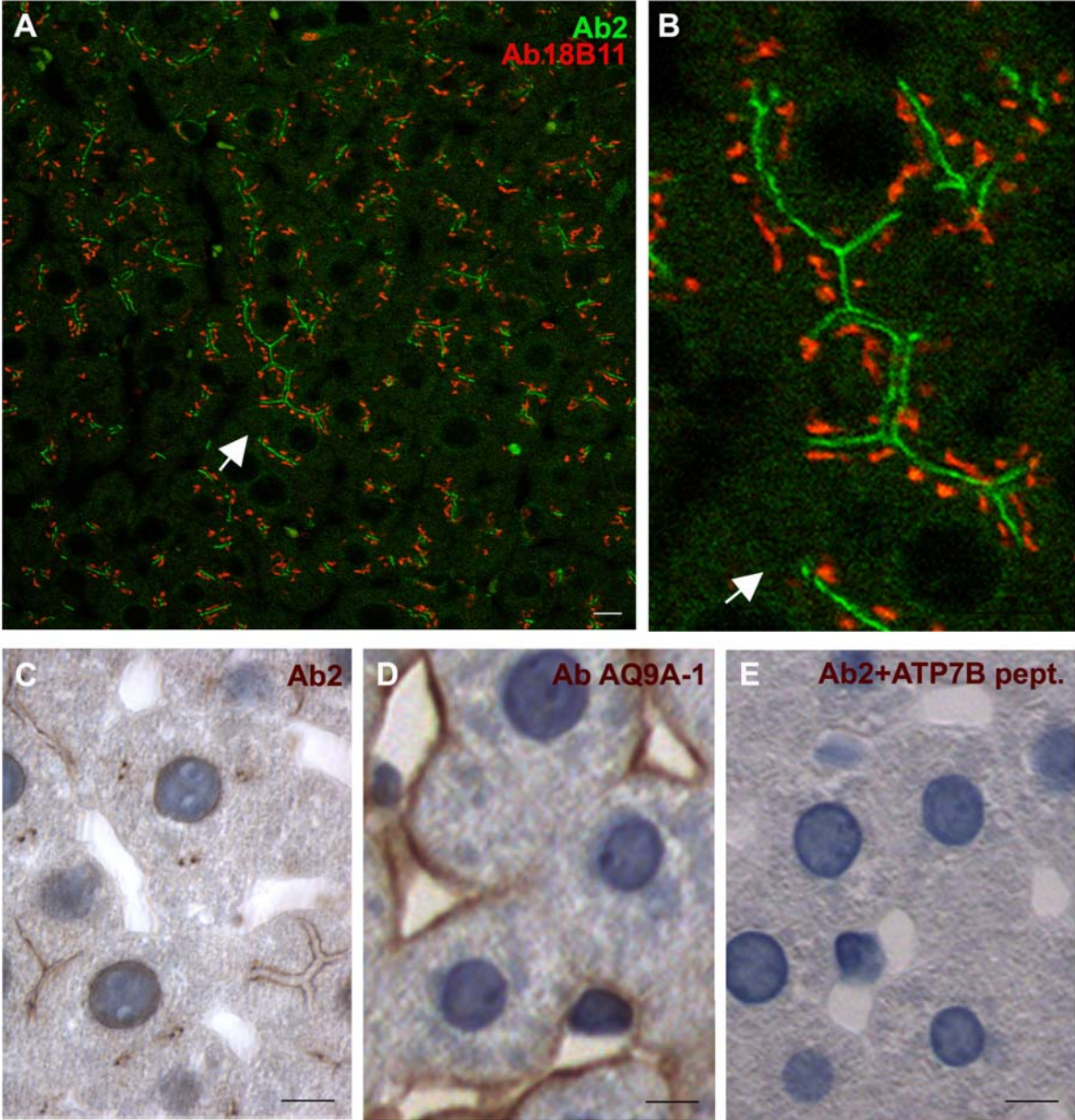


Figure 7

